High dielectric constant and nonlinear electric response in nonmetallic $YBa_2Cu_3O_{6+\delta}$

C. M. Rey, H. Mathias, and L. R. Testardi
Department of Physics, Florida State University, Tallahassee, Florida 32306

S. Skirius
Department of Chemistry, Florida State University, Tallahassee, Florida 32306
(Received 6 December 1991)

Dielectric constants from 10^2 to 10^6 are found in room-temperature, ceramic, nonmetallic $YBa_2Cu_3O_{6+\delta}$ ($\delta \sim 0$–0.4). The frequency, temperature, and electric-field dependencies of the dielectric response, as well as the quasistatic current-voltage behavior of this material, are reported. We show that the high polarizability is tied to a short (≤ 100 Å) length scale, persists to microwave frequencies, and is accompanied by a strong electric-field dependence.

I. INTRODUCTION

The oxygen-deficient precursor phase to high-temperature superconductivity in $YBa_2Cu_3O_7$ has been studied in the search for cooperative phenomena which may shed light on the mechanism of superconductivity. Dielectric constant measurements of ceramic, nonmetallic $YBa_2Cu_3O_{6+\delta}$ ($\delta \sim 0$–0.1) have been reported by Testardi *et al.*,[1] Jia and Anderson,[2] Behrooz and Zettl,[3] and Samara, Hammetter, and Ventunn,[4] and in other materials related to high-T_c superconductors by Varma *et al*,[5] Reagor *et al*,[6] and Emin and Hillery.[7] The possibility of ferroelectric-like instabilities related to superconductivity has been pointed out by Kurtz *et al.*,[8] Bussman-Holder, Simon, and Buttner,[9] Billesbach, Hardy, and Edwardson,[10] and Batistic *et al.*[11]

The experimental measurements often find high dielectric constants at low frequencies, but are generally at variance with each other by amounts far exceeding the estimated errors. The conclusion that the magnitude and the mechanism of the high dielectric constant depend upon an important unspecified state of the sample has led us to remeasure the dielectric response of $YBa_2Cu_3O_{6+\delta}$ and obtain more information on its electrical properties. We now find dielectric constants substantially larger than all previously reported work.

In this article we report the dc low electric-field conductivity, the nonlinear I-V characteristics, the real and imaginary parts of the dielectric constant and its electric-field dependence from 20 Hz to 1 MHz and from 0.2 to 20 GHz, all of which (except for the GHz measurements) have been performed over the temperature range 4.2–300 K. Characterization by x-ray diffraction, energy dispersive x-ray analysis (EDAX), scanning electron microscopy (SEM), and thermogravimetric analysis (TGA) have been obtained to help in identifying the microstate of these samples. SI units are used throughout this paper except where explicitly noted otherwise.

II. EXPERIMENT

A. Sample preparation

Two samples of $YBa_2Cu_3O_x$ identified as A and B were made with precalcined powder provided by W.R. Grace Co. The powder was made using a co-precipitation process which has been described in detail elsewhere.[12,13]

Prior to compaction of the disks, the precalcined powder was ball milled in an agate vial for 30 min by an 8000 Spex mixer mill. After mixing, the powder had a typical particle size between 5 and 10 μm. The two samples ($m \sim 10$ g) were pressed for ~ 30 min into 2.54-cm-(1-in.) diam disks under a compaction force > 25 tons.

The samples were then sintered together at 985 °C for 14 h under flowing O_2 (~ 50 cm^3/min). The temperature of the furnace was subsequently lowered to 515 °C at a rate of 1 °C/min. The temperature was held at 515 °C for 6 h in the same O_2 atmosphere. The samples were further furnace cooled to room temperature in 4 h.

The T_c of sample A was then measured using an ac inductance technique and showed an onset of 93 K with a transition width of 2 K. Beyond this point in the synthesis, two different processing paths (leading to samples A and B) were taken to simulate the variations in sample fabrication typically followed by workers in this field.

Sample A was reheated to 950 °C in flowing O_2 (~ 50 cm^3/min) in ~ 30 min, and held for 1 h at 950 °C. Sample B was reheated to 950 °C in flowing He (~ 50 cm^3/min) in 30 min, and held at 950 °C for 5 min. The samples were then quenched in deionized water from 950 °C to room temperature. Travel time from 950 °C to the water quench was < 2 sec. Sample A's density was then measured to be $\rho = 5.55$ g/cm^3 (90% theoretical for the 1236 structure), where $m = 9.193$ g, $d = 2.288$ cm, and $t = 0.403$ cm. Sample B's density prior to quenching was measured to be 6.25 g/cm^3 (98% theoretical density for 1237). For sample B the density after quenching was

measured to be 5.86 g/cm^3 (95% theoretical for 1236), where $m = 10.042$ g, $d = 2.306$ cm, and $t = 0.410$ cm.

Both samples were then dry polished using abrasion paper ranging from 120 to 400 grit followed by fine polishing on a wheel. At least one-third of a mm of outer material from the original water-quenched sample was removed in the polishing process.

Following the high-frequency (electrodeless) measurements, ultrasonically soldered indium-tin electrodes were established on the 1-in. faces of the disc-shaped samples whose thicknesses were now 2.49 mm (sample *A*) and 3.45 mm (sample *B*). These ultrasonically bonded electrodes are mechanically rugged and, when intentionally pulled to failure, will take a portion of the sample with them. Data collected through more than six temperature cycles (300-4.2-300 K) showed no change greater than 2% in 10 days.

B. Measurements

I-V and dc electrical conductivity measurements were made under computer control utilizing the HP 3458A Multimeter (with current specified resistance measurements and, for *I-V*, an independent current source. The low-frequency (≤ 1 MHz) dielectric measurements were made with an HP 4284A Precision LCR meter utilizing four coaxial lead measurement techniques which allow "open" and "short" corrected measurements of the sample up to 4 m (in LHe Dewar) away. The low-frequency dielectric constant was obtained from the measured complex admittance of the sample represented by capacitor and shunting admittance G via $Y = j\omega\epsilon_r^*\epsilon_0 A/t$, where ω is the angular frequency, A and t the sample area and thickness, ϵ_0 the electric permittivity of free space, $\epsilon_r^*(\omega) = \epsilon_r'(\omega) - \epsilon_r''(\omega)$ is the complex relative dielectric constant, $\epsilon_r''(\omega) = \sigma(\omega)/\omega\epsilon_0$ with $\sigma = t/AR$, and $R = 1/G$ is the equivalent parallel resistance.

High-frequency (0.2–20 GHz) measurements were made on nonelectroded samples utilizing an HP 8720B Network Analyzer and HP 85070A Dielectric Measurement Probe. This technique measures the S (scattering) parameters from an open-ended coaxial structure in whose fringe field the sample is located. No sample dimensions enter the data analysis with this method.

III. RESULTS

A. X-ray structure

Figure 1 shows the Cu $K\alpha$ x-ray-diffraction data for samples *A* and *B*. For sample *A* all lines with integrated intensities greater than 5% of the strongest line can be indexed on a tetragonal structure with $a = 3.865$ Å and $c = 11.69$ Å (see Table I). For sample *B* almost all lines can be indexed to a tetragonal structure with $a = 3.862$ Å and $c = 11.840$ Å. The main exception, in the latter case, occurs at $2\theta = 29.8°$ with an intensity of 5%–10% of the main peak, and which could be indexed as a 2:1:1 phase. The observed intensities for the tetragonal 1:2:3 phase lines are generally in approximate (±30%) agreement with those calculated for a random orientation of this

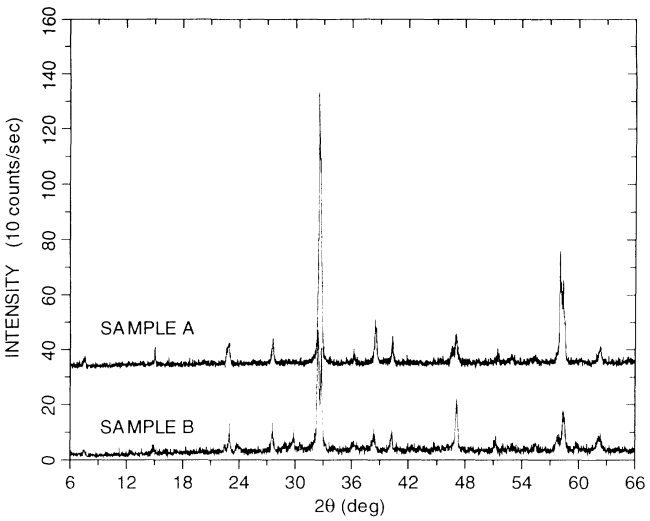

FIG. 1. X-ray-diffraction intensity vs 2θ (Cu $K\alpha$ radiation) for samples *A* and *B*.

known structure.[14] The results of the x-ray analysis show that there is little difference (~0.1%) in the a parameters for these samples, or in their values as compared with previously[14] reported work for this phase. The major difference lies in the c parameters which differ by 1.2% and which values fall somewhat outside the range 11.74 Å (for $\delta \sim 0.4$) to 11.82 Å (for $\delta \sim 0$) published[14] for the room-temperature structure of $YBa_2Cu_3O_{6+\delta}$. We will show below that both samples exhibit high dielectric constants but with substantial differences at the higher frequencies studied.

B. Microstructure and composition

The microstructures of samples *A* and *B* and their elemental composition were obtained from SEM and EDAX analysis. The main distinguishing feature in microstructure lies in the occurrence in sample *A* of contrasting "rivers" whose width is ~0.1 mm and whose two-dimensional area occupies several percentages of the sample area. EDAX measurements show that both samples have average atomic ratios Y:Ba:Cu which are 1:2:3 to within the 5% uncertainty of the measurements. The "rivers" in sample *A*, however, are Y poor with atomic ratios 0.3:2:3. We discuss below the possible effects of this inhomogeneity on the conductivity and dielectric response of sample *A*. No such structure is found in sample *B*.

Figure 2 shows thermogravimetric data for the mass gain of sample *B* (after all measurements reported below) heated in flowing O_2 to 950 °C followed by cooldown under programmed rates as shown in the figure. A mass gain of 2.4% is found on initial heating to 550 °C followed by unloading and reloading on cooling to a final (superconducting phase) state whose mass gain is ≈2% from the starting (dielectric measurement) state. This change corresponds to an increase in δ of 0.8 ± 0.1 for the formula $YBa_2Cu_3O_{6+\delta}$ between the measured phase and the superconducting phase. If, in addition, the final (supercon-

TABLE I. X-ray-diffraction data.

2θ (deg. approx.)	Reflection	Sample A d (obser.)	Sample A d (pred.)[b]	Sample B d (obser.)	Sample B d (pred.)[c]
7.5	001	11.56	11.70	11.84	11.84
15.0	002	5.840	5.85	5.659	5.920
22.5	003	3.907	3.900	3.959	3.950
23.0	100	3.871	3.865	3.857	3.862
32.4	103	2.743	2.745	2.761	2.760
32.7	110	2.730	2.733	2.730	2.731
38.6	005	2.339	2.339	2.350	2.368
40.2	113	2.237	2.238	2.241	2.246
46.2	006	1.949	1.949	1.971	1.973
47.0	200	1.933	1.933	1.932	1.931
51.2	115	1.777	1.777	1.790	1.789
57.8	116	1.589	1.587	1.597	1.599
58.3	123	1.581	1.580	1.582	1.582
68.6	220	1.367	1.367	1.365	1.365

[a]Cu $K\alpha$ radiation.
[b]$a=b=3.865$ Å, $c=11.696$ Å.
[c]$a=b=3.862$ Å, $c=11.840$ Å.

ducting) phase has $\delta\sim 0.9-1.0$, then the initial δ had values in the range 0.1–0.2. The initial loading corresponds to a gain in δ of 1.0 ± 0.1 and, assuming a final state $\delta=0.9-1.0$, would correspond to the loading peak value of $\delta=1.1-1.2$. These values are within the range of expectation, and differ by no more than 0.1 from those estimated by Samara, Hammetter, and Venturin[4] for the samples of their dielectric measurements. For sample A, the mass gain is smaller and a similar argument leads to $\delta\sim 0.4\pm 0.1$. Thus, by TGA and unit-cell size, sample A is closer to the phase boundary separating the semiconducting and superconducting states.

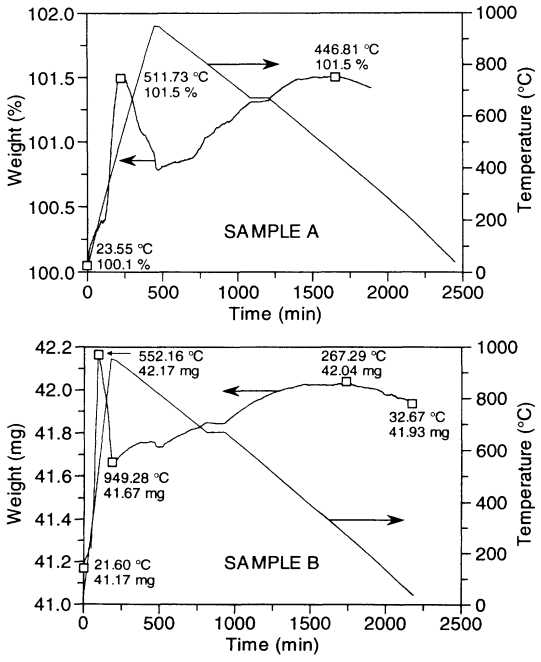

FIG. 2. Sample weight vs time from thermogravimetric analysis (TGA). Upper part for sample A and lower part for sample B.

C. dc conductivity

Figure 3 shows the quasistatic (~1 sec/sweep) current density J vs electric-field E behavior for both samples at

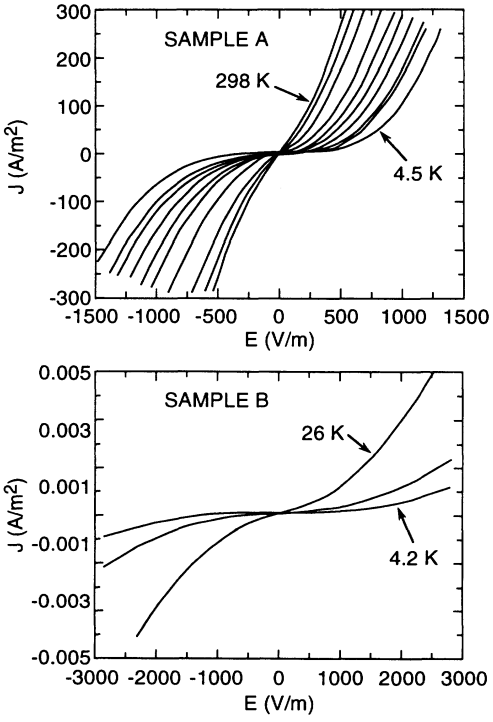

FIG. 3. Current density J vs electric field E at various temperatures. Upper part for sample A at temperatures 4.5, 27, 44, 85, 124, 154, 200, 249, 278, and 298 K, and at lower part for sample B at temperatures 4.2, 15, and 26 K.

various temperatures. A substantial nonlinear relation, but of different magnitude, is found in both cases at almost all temperatures and at the modest electric fields of 10^2-10^3 V/m. Since many measurements and devices default to signal levels ~ 1 v, the use of samples less than or equal to several mm in thickness can be accompanied by a large nonlinear response whose effect upon a circuit expecting linear response will be device dependent and largely unpredictable.

The source of this unusually large nonlinear conduction has not been identified, although one conceivable mechanism deserves further discussion. The possibility of Schottky-type barriers at the electrodes is discounted by noting the symmetry and shape of the J-E behavior. Since $J(E)=-J(-E)$, any asymmetric Schottky contact effect would have to occur with equal strength at each contact. Because the contacts are in series, the impedance Z would be dominated by the "reverse" (large-Z) characteristic which should show current saturation with increasing V. The odd symmetry J vs E and the increasing conductance with increasing E in both directions would represent behavior contrary to expectations for Schottky or p-n junctions.

Because of this strongly nonlinear J vs E behavior, all measurements of the conductivity and the dielectric response were made with E fields ≤ 2 V/m or with larger-E fields accompanied by experimental confirmation that such results were E field independent.

Figure 4 shows the low-E field conductivity of both samples as a function of temperature. Sample A exhibits the unusual behavior $\sigma=\sigma_0\exp(T/T_0)$, where $\sigma_0=1.3\times10^{-3}$ S and $T_0=55$ K as qualitatively found previously.[15] This is wholly different then, and in no way describable by, the conductivity for a thermally activated process where the exponent, T_A/T, would be inversely related to temperature. Sample B has $\sigma(T)$ which is not given by either relation over the entire temperature range.

Note that the room-temperature resistivities [$\rho(A)\sim250$ Ω cm and $\rho(B)\sim500$ Ω cm] are within the range ($\times2$) usually cited for the tetragonal phase and as found, for example, in the work of Samara *et al.*[4]

D. Low-frequency dielectric response

The central result of the dielectric studies, which is the occurrence of high dielectric constants in the semiconducting phase of 1:2:3, is presented in Fig. 5. Note that, in these room-temperature data, both samples show real dielectric constants $\epsilon_r'\sim10^6$ at the lowest frequencies. These are accompanied by large imaginary components ϵ_r'' such that the dissipation factor $D\equiv\epsilon_r''/\epsilon_r'\sim10^2$ for $\omega/2\pi=f<10^2$ Hz.[16] We will show shortly, however, that the large dissipation at low frequencies is directly the result of the dc conductivity.

At higher frequencies a larger difference develops between the ϵ's of the two samples. For 10^5-10^6 Hz, the real dielectric constants differ by $\sim10^2$ although both are large ($\epsilon_r'\sim10^5$ for sample A and $\sim10^3$ for sample B) and D for the larger ϵ_r' (sample A) is now <1.

Figures 6 and 7 (upper) show the frequency-dependent conductivities for the two samples. Note that both reach limiting values at low frequencies given by $\sigma_A\rightarrow0.47$ S

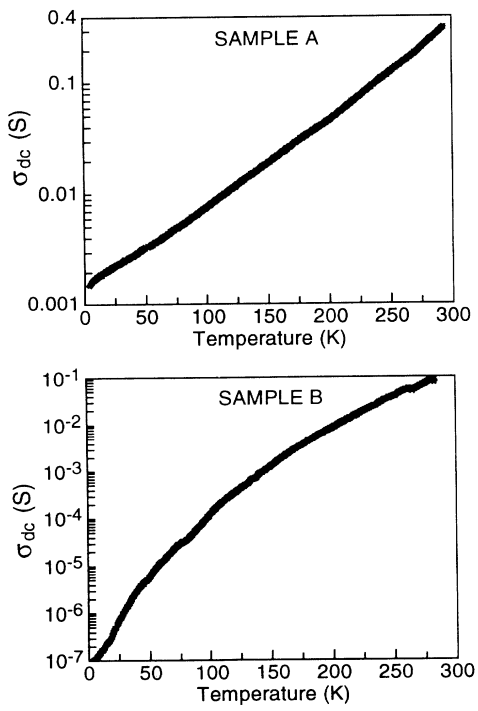

FIG. 4. Low-E field dc electric conductivity vs temperature. Upper part, sample A, and lower part, sample B.

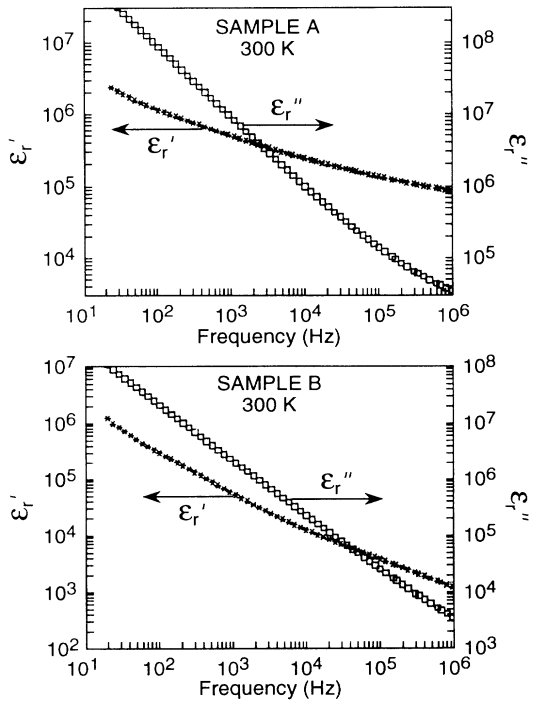

Fig. 5. Real and imaginary relative dielectric constants vs frequency at 300 K. Upper part, sample A; and lower part, sample B.

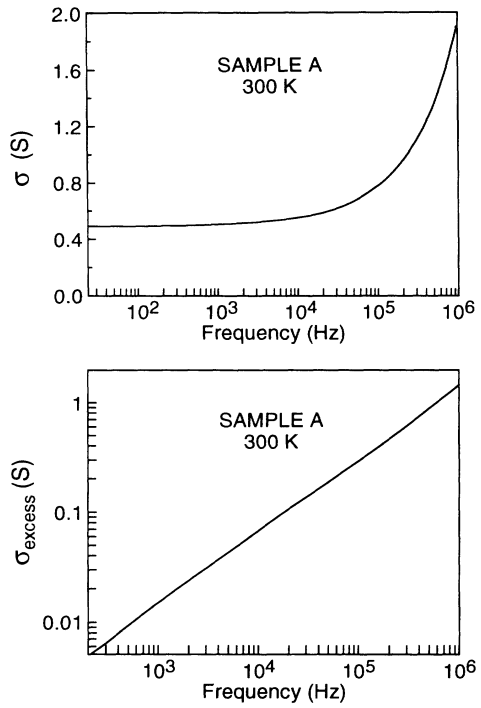

FIG. 6. Upper part, electrical conductivity $\sigma(\omega)$; and lower part, excess electrical conductivity $\sigma(\omega)$-$\sigma(0)$ vs frequency at 300 K for sample A.

and $\sigma_B \rightarrow 0.125$ S. These (small-signal) ac values are in reasonable agreement with the independent low-E field measurements of the dc conductivity ($\sigma_A \sim 0.45$ S and $\sigma_B \sim 0.13$ S) shown in Fig. 4. Thus, the high dielectric dissipation is wholly related to dc conduction at frequency $< 10^2 - 10^3$ Hz.

At higher frequencies the conductivity increases rapidly. We represent this frequency-dependent contribution using the relation

$$\sigma(\omega) = \sigma(0) + \sigma_{\text{excess}} \tag{1}$$

and display $\log_{10}(\sigma_{\text{excess}})$ vs $\log_{10}(f)$ in the bottom parts of Figs. 6 and 7. For example A, σ_{excess} accurately follows f^n with $n = \frac{2}{3}$ for nearly 4 orders of magnitude in f. For sample B, the power-law dependence is seen only over $10^3 - 10^6$ Hz and with $n = 0.43$.

The temperature dependencies of the dielectric constants for these two samples show a greater divergence at lower temperatures. Figure 8 shows the behavior of ϵ_r' and ϵ_r'' at 1 MHz from 4 to 300 K. These low-E field (< 2 V/m) measurements show that ϵ_r' decreases rapidly to lower values at lower temperatures for sample B. For sample A, however, the decrease is slower and, given the larger value at 300 K, ϵ_r' still exceeds 10^4 with $D < 0.2$ at 20 K.

The conductivity at this frequency, given in Fig. 9, shows different behavior again for the two samples. For both samples, in addition, the conductivities (i) do not show the temperature-activated process behavior, (ii) show far less T dependence than the dc conductivity and,

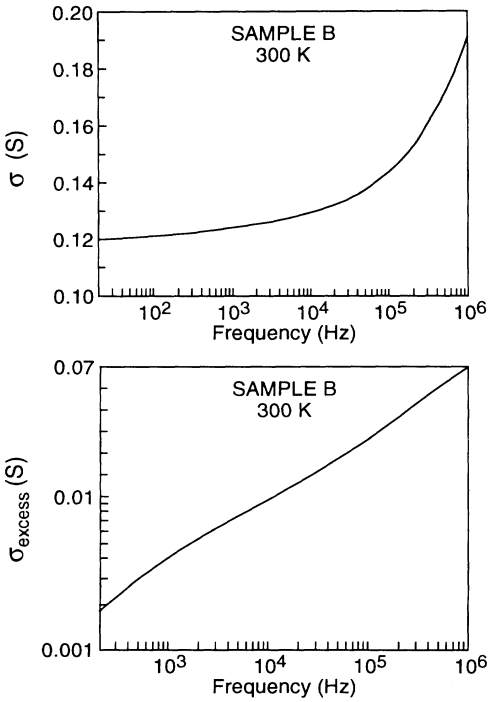

FIG. 7. Upper part, electrical conductivity $\sigma(\omega)$; and lower part, excess electrical conductivity $\sigma(\omega)$-$\sigma(0)$ vs frequency at 300 K for sample B.

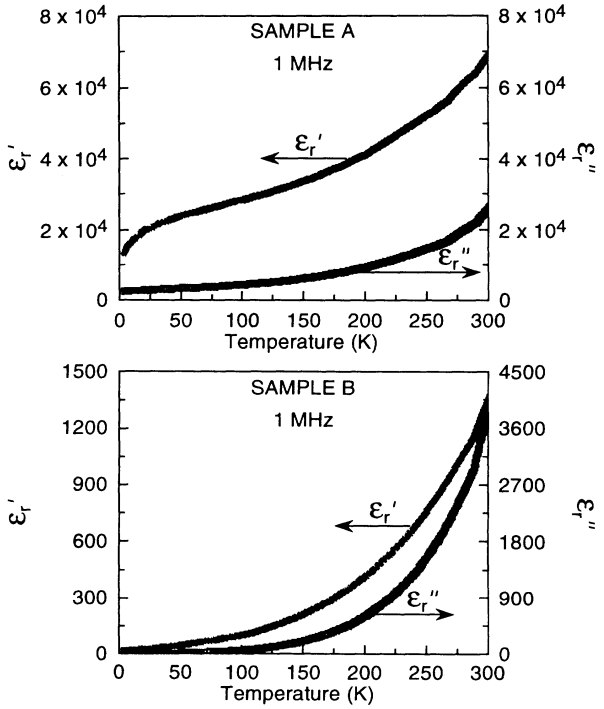

FIG. 8. Real and imaginary relative dielectric constants at 1 MHz vs temperature. Upper part, sample A; and lower part, sample B.

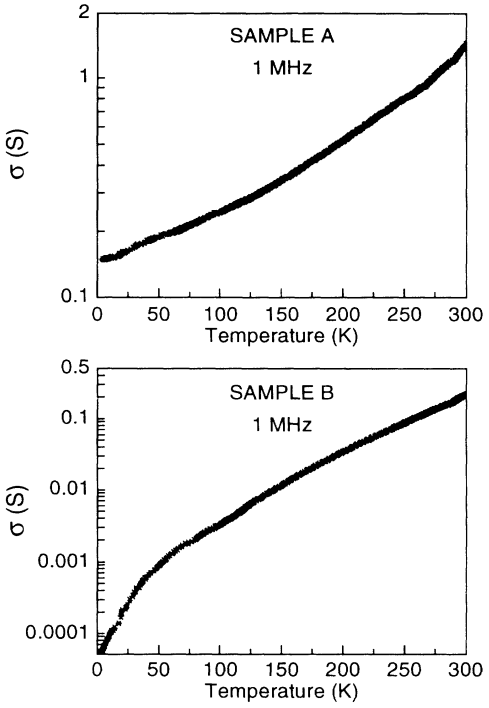

FIG. 9. Electrical conductivity σ (1 MHz) vs temperature. Upper part, sample A; and lower part, sample B.

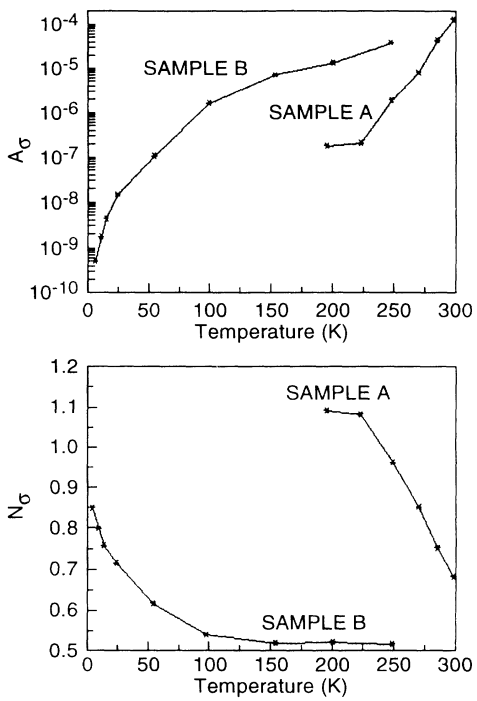

FIG. 10. The quantities A_σ (upper part) and N_σ (lower part) from Eq. (3) vs temperature for samples A and B.

(iii) show a rough $\sigma(\omega) \propto \exp(T/T_0)$ behavior between 100 and 300 K.

To give a fuller, but concise, description of the temperature dependence, we have analyzed the frequency dependence of ϵ_r' and ϵ_r'' over the range 10^3–10^6 Hz in the forms

$$\epsilon_r' = A_\epsilon f^{N\epsilon} , \tag{2}$$

$$\sigma = A_\sigma f^{N\sigma} . \tag{3}$$

The temperature dependence of the dielectric behavior between 10^3 and 10^6 Hz, given in terms of A_ϵ, A_σ, N_ϵ, and N_σ vs temperature (with f in Hz), is given in Figs. 10 and 11 for both sample A and sample B. No values are shown for these temperatures where the power-law behavior of Eqs. (2) and (3) does not hold.

As pointed out by Samara, Hammetter, and Venturin,[4] Kramers-Kronig relations requiring $N_\sigma = N_\epsilon + 1$ and $4\pi\epsilon_0 A_\epsilon / A_\sigma = \tan(N_\sigma \pi/2)$ will apply, but provided that (i) Eqs. (2) and (3) are valid over a wide range of frequency and (ii) the system is measured in the region of linear response. The experimental relation $N_\sigma = N_\epsilon + (0.8-1.2)$ for both samples through a portion of the temperature range indicates that, even in the restricted T range, at least one of the above conditions is not precisely satisfied. A discrepancy of similar magnitude is found in A_ϵ / A_σ. In view of the independent test of linear dielectric response, the power laws of Eqs. (2) and (3) are, therefore, only an approximation. Further evidence of this is given below.

The dc E field dependence of the complex dielectric constant was measured utilizing small-signal ac measurements ($E_{ac} < 2$ V/m) to remain in the linear response region combined with dc fields E_{dc} up to 500 V/m. The results, shown in Fig. 12 for the 1-MHz room-temperature data, indicate a large reduction in the real dielectric constant, and a large increase in dissipation with very modest

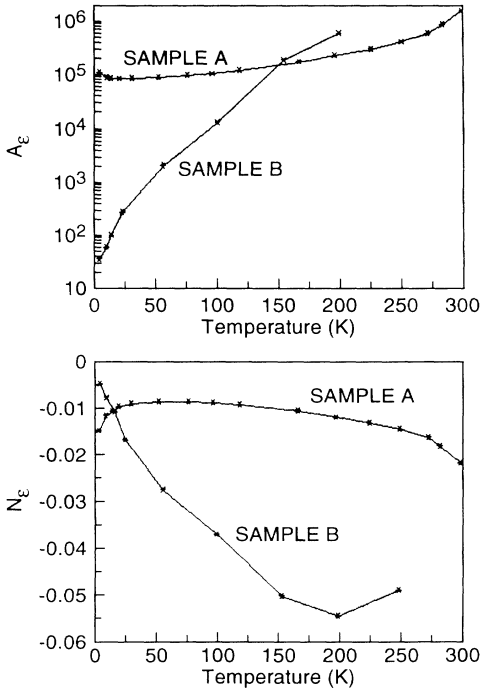

FIG. 11. The quantities A_ϵ (upper part) and N_ϵ (lower part) from Eq. (2) vs temperature for samples A and B.

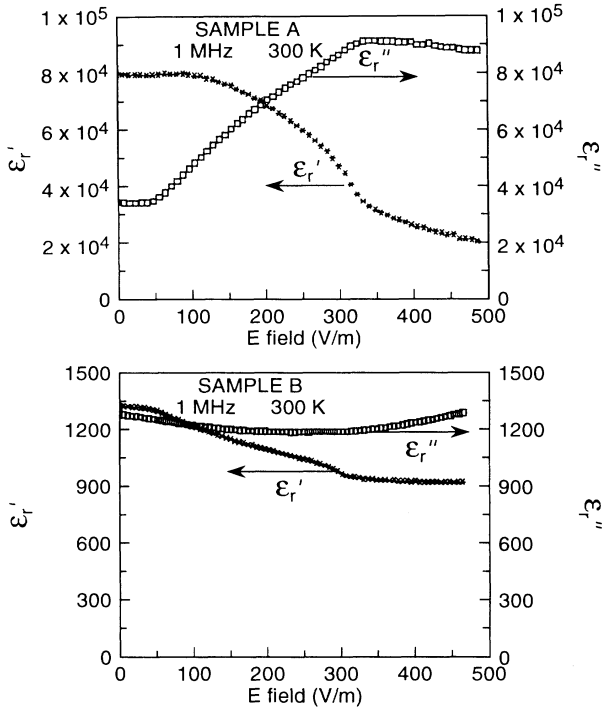

FIG. 12. Real and imaginary relative dielectric constant at 1 MHz and 300 K vs E field bias. Upper part, sample A, and lower part, sample B.

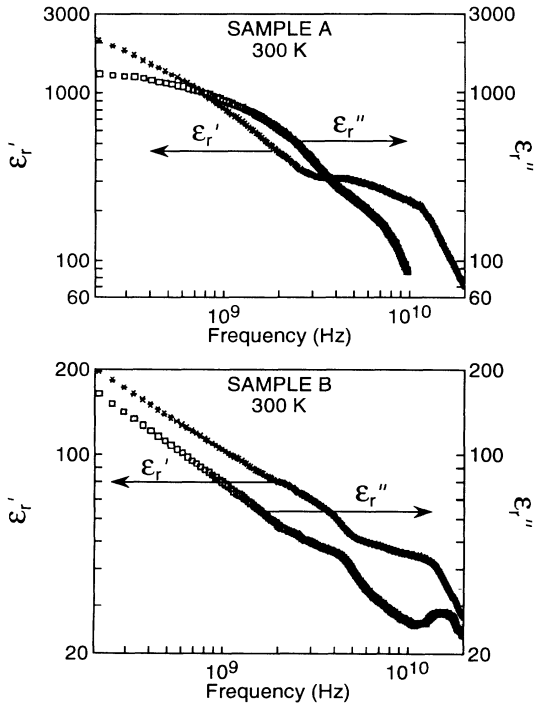

FIG. 13. Real and imaginary relative dielectric constant at 300 K vs frequency. Upper part, sample A; and lower part, sample B.

E fields, reminiscent of that found in the dc conductivity. Though not further described here, this E field dependence of ϵ_r' diminished with decreasing frequency where ϵ_r' increases, and diminished with decreasing temperature where ϵ_r' decreases. Thus, the strong field dependence does not simply correlate with the (anomolously high) magnitude of ϵ_r'.

E. High-frequency dielectric response

The real and imaginary parts of the dielectric response for samples A and B at 300 K, obtained from 0.2 GHz to 20 GHz, are given in Fig. 13. Note that ϵ_r' is quite large (>70) for sample A throughout this microwave region of the spectrum. The extrapolation of Eqs. (2) and (3) to the microwave region leads to values of ϵ_r' at 0.2 GHz $\sim 2\times 10^4$ (beyond the measurement ability) for sample A and ~ 70 for sample B. The discrepancy with the measured values is an indication of the (not surprising) failure of Eqs. (2) and (3) over range of frequency.

The occurrence of high dielectric constants for both samples in these data indicates, of course, that the source of the polariziblity has not been exhausted at these high frequencies. More important, it also shows that it does not come from the indium soldered contacts (via Schottky-barrier effects) used in the low-frequency measurements, since the high-frequency measurements are made with electrodeless samples.

F. Discussion

There is little doubt that large capacitances are associated with these samples. For sample A, with a thickness of 2.49 mm and a diameter of 2.54 cm, the measured values at 300 K range from 5.2 μF ($\sim 10^{-2}$ F/m^2) at 20 Hz to 0.16 μF ($\sim 3\times 10^{-4}$ F/m^2) at 1 MHz. The measurement error, obtained by independent "in-place substitution" calibration using known standards of matched complex impedance, is $\leq 5\%$ at all frequencies for the (real) capacitance, and substantially smaller for the dissipation up to 10^5 Hz.

The derived large dielectric constant, however, assumes a homogeneous (uniform displacement field) sample via the use of the sample thickness for the low-frequency data. This may be viewed as an incorrect assertion leading to the large values of ϵ_r'. In the classic Maxwell-Wagner mechanism for inhomogeneity enhanced dielectric constants, the electric displacement occurs over only a small fractional length f_i of the sample due to its much lower electrical conductivity (but not comparably smaller dielectric constant) compared to the major portion of the sample. In its simplest manifestation, which also yields the greatest enhancement in ϵ_r', the inferred dielectric constant for $\omega \to 0$ will be ϵ_r'/f_i for $\sigma_i \ll \sigma_b$ and $f_i \ll 1$, and where i refers to the thin low conductivity layer in the bulk material b. Assuming only typical values for $\epsilon_i' \sim 10$ and the limiting low-frequency value $\epsilon_r' > 2\times 10^6$ obtained here then leads to $f_i \leq 5\times 10^{-6}$. Since the sample thickness is $\sim 2\times 10^{-3}$ m, the total thickness of all i layers must be ≤ 100 Å. Furthermore, the observed ϵ_r' were obtained, in this case,

with bias voltages of ~ 1 V, and thus the insulating layer must also sustain an E field $\geq 10^8$ V/m, which is relatively high for a solid.

An additional and more serious problem with this explanation is that the one-dimensional inhomogeneity model used above topologically demands that this layer intercept all D fields lines. For inhomogeneity in the form of spherical inclusions, as might be expected for powder processed material, the Maxwell-Wagner effect, as calculated by Hanai,[17,18] will provide far less enhancement to ϵ_r'. The one-dimensional inhomogeneity (Y-poor "rivers") found in sample A is also of a geometry which would not lead to a large Maxwell-Wagner effect for the composite dielectric constant since the D fields are, again, not constrained to pass through the inhomogeneity.[20]

Finally, the rapid variation of the displacement field over a short distance must, by Maxwell's equations, be accompanied by a volume charge density. For a spatially constant charge density, a dielectric constant $\epsilon_i'=10$, and a contact potential difference to the neighboring material of ~ 1 V, the required charge density[19] is $>10^{19}$ cm^3. This would be large for an insulator whose conductivity σ_i must be $\leq f_i \sigma_{\text{measured}} \sim 10^{-6}$ S.

It is thus difficult to find an explanation for the high dielectric constant based on inhomogeneity without invoking a length scale finer than expected from processing, and approaching that of a single layer of ≤ 8 unit cells traversing, continuously, the entire cross section of the sample. This region, in addition, must retain the character of very high breakdown voltage and very low conductivity not withstanding the large charge density within it required by Maxwell's equations. These large dielectric constants cannot, in addition, result from insulating layers of ordinary ϵ' and thickness d_i surrounding grains or incompletely sintered particles of dimension $d_i \sim 10$ μm (for example), in part, because the topology would not allow it, but also because $d_i \approx d_b f_i = d_b(10^{-6}\epsilon_i')$ would then be <1 Å. Thus, one is driven to a length scale so fine that its distinction from the homogeneous state is arbitrary.

It is equally important, however, to note that a great variation in the dielectric response has been reported by different investigators. Some, though certainly not all, of this difference may be due to inequivalent measurement conditions. There remains a large discrepancy that must be attributed to sample differences. In this paper we have identified the processing, microstate, and properties of our sample better than previously done. We have found that sample A, which, by x ray, TGA, and electrical conductivity, is closer to the semiconductor-superconductor phase boundary, also has the higher dielectric constant and greater field dependence of ϵ and σ. But, while some differences in our samples have been established, we have not found that characteristic which is a clear predictor of the dielectric behavior. More important, perhaps, is the continued observation of (now even larger) high dielectric constants, accompanied by large, nonlinear E field dependencies of the conductivity and dielectric response, which lie close by the superconducting phase.

ACKNOWLEDGMENTS

The authors wish to thank William Jenks for assistance in the dielectric measurements, Tom Fellers for the SEM analysis, and the Defense Advanced Projects Research Agency for their financial support of the Florida Advanced Microelectronics and Materials Program.

[1] L. R. Testardi, W. G. Moulton, H. Mathias, H. K. Ng, and C. M. Rey, Phys. Rev. B **37**, 2324 (1988).
[2] Q. X. Jia and W. A. Anderson, J. Appl. Phys. **66**, 452 (1989).
[3] A. Behrooz and A. Zettl, Solid State Commun. **70**, 1059 (1989).
[4] G. A. Samara, W. F. Hammetter, and E. L. Venturin, Phys. Rev. B **41**, 8974 (1990).
[5] K. B. R. Varma, G. N. Subbana, T. V. Ramukrishnan, and C. N. R. Rao, Appl. Phys. Lett. **55**, 75 (1989).
[6] D. Reagor, E. Ahrens, S-W. Cheong, A. Migliori, and Z. Fisk, Phys. Rev. Lett. **62**, 2048 (1990).
[7] D. Emin and M. S. Hillery, Phys. Rev. B **39**, 6575 (1989).
[8] S. K. Kurtz, L. E. Cross, N. Setter, D. Knight, A. Bhalla, W. W. Cao, and W. N. Lawless, Mater. Lett. **6**, 317 (1988); S. K. Kurtz, J. R. Hardy, and J. W. Flocken, Ferroelectrics **87**, 29 (1988).
[9] A. Bussmann-Holder, A. Simon, and H. Buttner, Phys. Rev. B **39**, 207 (1989).
[10] D. P. Billesbach, J. R. Hardy, and P. J. Edwardson, Phys. Rev. B **39**, 202 (1989).
[11] I. Batistić, A. R. Bishop, R. L. Martin, and Z. Tešanović, Phys. Rev. B **40**, 6896 (1989).
[12] N. D. Spencer, W. H. Pan, and J. A. Rudesil, European Patent Application No. 0306876.
[13] N. D. Spencer, T. S. Pedars, and M. B. Bear, J. Mater. Res. **6**, (1991).
[14] See, for example, the review of 1:2:3 crystal structures by R. M. Hazen, in *Physical Properties of High Temperature Superconductors II,* edited by D. M. Ginsberg (World Scientific, Singapore, 1990), pp. 139–143.
[15] L. R. Testardi, W. G. Moulton, H. Mathias, H. K. Ng, and C. M. Rey, Phys. Rev. B **36**, 8816 (1987).
[16] An independent test of the accuracy of the HP 4284A LCR meter was made using known components that simulate the impedances reflected in Fig. 4. These results shown that C (and ϵ_r') are obtained to within $\sim 5\%$ for $D=100$, and 0.5% for $D=10$.
[17] For an excellent discussion of the Maxwell-Wagner effect, see A. von Hippel, *Dielectric and Waves* (Wiley, New York, 1954), pp. 228–231.
[18] T. Hanai, Kolloid Z. **171**, 23 (1960); Bull. Inst. Chem. Res. Kyoto Univ. **39**, 341 (1961).
[19] See, for example, J. H. Shine, *The Properties, Physics and Design of Semiconductor Devices* (Van Nostrand, New York, 1959), pp. 359–361.
[20] If the "rivers" have electrical conductivity high compared with the bulk, this inhomogeneity can lead to an increase in σ and ϵ_r'' for sample A, of course.